A Proposed ANN-Based Acceleration Control Scheme for Soft Starting Induction Motor

AMIR ABDEL MENAEM[1,2], MOHAMED ELGAMAL[1], (Graduate Student Member, IEEE), ABDEL-HALEEM ABDEL-ATY[3], EMAD E. MAHMOUD[4], ZHE CHEN[5], (Fellow, IEEE), AND MOHAMED A. HASSAN[1,6], (Member, IEEE)

[1]Electrical Engineering Department, Faculty of Engineering, Mansoura University, Mansoura 35516, Egypt
[2]Department of Automated Electrical Systems, Ural Power Engineering Institute, Ural Federal University, 620002 Yekaterinburg, Russia
[3]Department of Physics, College of Sciences, University of Bisha, Bisha 61922, Saudi Arabia
[4]Department of Mathematics and Statistics, College of Science, Taif University, Taif 21944, Saudi Arabia
[5]Department of Energy Technology, Aalborg University, DK-9220 Aalborg, Denmark
[6]Center for Engineering Research, Research Institute, King Fahd University of Petroleum and Minerals, Dhahran 31261, Saudi Arabia

Corresponding author: Amir Abdel Menaem (ashassan@mans.edu.eg)

ABSTRACT In this article, a new soft starting control scheme based on an artificial neural network (ANN) is presented for a three-phase induction motor (IM) drive system. The main task of the control scheme is to keep the accelerating torque constant at a level based on the value of reference acceleration. This is accomplished by the proper choice of the firing angles of thyristors in the soft starter. Using the ANN approach, the complexity of the online determination of the thyristors firing angles is resolved. The IM torque-speed characteristic curves are firstly used to train the ANN model. Secondly, the IM- soft starter system is modeled using MATLAB/SIMULINK. To prove the effectiveness of the proposed ANN-based acceleration control scheme, different reference accelerations and loading conditions are applied and investigated. Finally, a laboratory prototype of 3 kW soft starter is implemented. The proposed control scheme is executed in a real-time environment using a digital signal processor (Model: TMS320F28335). The simulation and real-time results significantly confirm that the proposed controller can efficiently reduce the IM starting current and torque pulsations. This in turn ensures a smooth acceleration of the IM during the starting process. Moreover, the proposed control scheme has the superiority over several soft starting control schemes since it has a simple control circuit configuration, less required sensors, and low computational burden of the control algorithm.

INDEX TERMS Acceleration control, artificial neural network, digital signal processing, induction motors.

I. INTRODUCTION

Induction motors (IMs) are widely used in the electrical drive systems such as fans and pump drives [1]. A simple structure, lower costs, good mechanical properties, and easy operation and maintenance are the main advantages of IMs [2]. On the other hand, IMs have major challenges such as large accelerating torque and high starting currents. With the large accelerating torque, the motor is rapidly accelerated to the full load motor speed threatening the safety of the load operation. It may cause pressure surges in the pump applications. Conveyor belt systems could be endangered by jerking and stresses on the drive components like gears and chains.

The associate editor coordinating the review of this manuscript and approving it for publication was Paolo Giangrande.

Fans and/or systems with belt drives may be exposed to belt slippage [3], [4]. In addition, high starting currents heat the motor windings, stress the motor bearings and insulations, create a sharp decline in the grid voltage and generate electrical fluctuations during the starting process [5]. A proper starting scheme is needed to overcome these problems. Reduced voltage starting, variable frequency drive starting, and the solid-state or electronic reduced voltage (soft starter) technique are the main starting schemes [1]–[5]. A soft starter scheme has several advantages compared with several starting schemes. It has high effectiveness and low cost [5]–[9]. The soft starter mainly consists of a set of back-to-back thyristors connected with stator motor windings. The IM voltage is controlled by adjusting the firing angle with respect to the zero crossing of the supply voltage.

To reduce the accelerating torque and starting current, three soft starter techniques were implemented: voltage-ramp technique [1], [10], [11], current control technique [12]–[23] and torque control technique [24]–[26]. Voltage-ramp technique is widely used in the commercial soft starters. The IM terminal voltage is gradually increased by decreasing the firing angle of the thyristors until the rated voltage is reached. It does not guarantee an effective current and acceleration control during the starting process. To overcome the technique's defects, current and torque control techniques are suggested. The current control techniques keep the motor line's current constant at a pre-set value throughout the starting time [12]–[14]. If the feedback motor is lower than the pre-set value, the firing angle is decreased based on cosine [12], exponential [13], or ramp [14] time functions. Otherwise, the controller sets the firing angle constant to return the motor line's current to the pre-set value.

Classic controllers such as proportional-integral (PI) and proportional–integral–derivative (PID) controllers are investigated for the purposes of current [14], [15] and torque control [24]. Tuning the controller parameters by a trial-and-error method is a challenge in practice [14]. Adaptive optimization algorithms are proposed to tune the PI controller parameters [16]–[21]. Ant colony optimization (ACO) [16], genetic algorithm (GA) [17], particle swarm optimization (PSO) [18], [19], cuckoo search and bat algorithms [20], and flower pollination algorithm [21] are used to optimally design the controller parameters. A high computational burden in firing angle estimation is needed for a classic controller. Moreover, a feedback from the motor current or estimated torque is needed. An artificial neural network (ANN) and adaptive neuro-fuzzy inference system (ANFIS) are used to adapt the firing angles in the current [22], [23] and torque control techniques [25], [26] to overcome the classic soft starter controller problems. A closed loop fuzzy soft starter controller is proposed to adjust the firing angle based on the motor current deviation and deviation rate [22]. Using a two neural network (NN) controller, the current control technique is studied [23]. The first NN characterizes the relation between the thyristors firing angle and motor current. While the second NN controller adjusts the firing angle based on the error between the reference value from the first NN and the actual feedback current. ANN and ANFIS are implemented to estimate the firing angle profile in the torque control technique [25], [26]. Depending on the motor voltages and currents measurements, the motor torque is estimated using ANN [25] or ANFIS [26]. The estimated motor torque and reference speed values are combined to determine the firing angle. Even though the complexity of the firing angle computation is solved using intelligent controllers, the results are not satisfactory. Moreover, intelligent controllers operate in a closed loop and hence occupy a high number of voltage and current sensors making the control circuit more complex and expensive.

To overcome the aforementioned shortcomings of the IM soft starters, this article proposes a new ANN-based acceleration control scheme. The proposed control scheme governs the motor torque to follow the load torque variation keeping the motor acceleration constant at a normal level. Thus, the IM is started smoothly without any mechanical stress on the drive components ensuring safety operation of different industrial loads like pumps, compressors, fans, blowers, and grinders. In addition, employing motor acceleration as a control parameter leads to an open-loop control configuration. Few sensors are needed since there is no need for the motor current or estimated torque feedback. Moreover, ANN is used to resolve the complexity of the online determination of the appropriate thyristors firing angles. The challenges of tuning the PI controller parameters and testing different time functions of firing angle variation are settled. Since the ANN performance depends on the accuracy of the trained data sets, a well deducted characteristic curves of the motor performance are obligatory during the starting period.

The workflow can be summarized as follows:

1) Analyzing the operation modes of the soft starter fed IM.
2) Deducing the torque-speed characteristic curves of the IM with different firing angles.
3) Developing the training of the ANN model based on the deduced data sets.
4) Developing a SIMULINK model and get the simulation results.
5) Implementing an experimental prototype to prove the practical superiority of the proposed technique.

This article is structured as follows. After a brief introduction, the principle of operation of the soft starter is introduced in section II. Section III illustrates the ANN-based soft starter controller. Section IV describes the IM- soft starter system. Section V explains the SIMULINK model and simulation results. Section VI depicts the experimental work and real-time results. Results discussion and comparison with previous works are demonstrated in section VII. Section VIII outlines the main findings.

II. MATHEMATICAL MODEL OF SOFT STARTER
In the soft starter, The IM terminal voltage is controlled by adjusting the thyristors firing angle (α) with respect to the zero crossing of the supply voltage. Depending on the firing angle, the IM operates in one of three operation modes: three-phase, two-phase, or no-phase. In the natural sinusoidal operation, the firing angle should be set below the power factor angle (θ) of the motor [12]. If $\alpha > \theta$, the motor starts operating in the non-sinusoidal operation modes; two-phase/three-phase (2/3) and no-phase/two-phase (0/2). To obtain the relationship between the firing angle and stator current or torque, the single-phase IM equivalent circuit is simplified by finding the Thevenin equivalent circuit as shown in Figs. 1-a & 1-b. From (1) and (2), Thevenin voltage (V_r) and Thevenin reactance (X) between nodes c & d are determined. The stator current (I_s) depends mainly on the terminal phase voltage (V_t) and Thevenin equivalent voltage (V_r) as
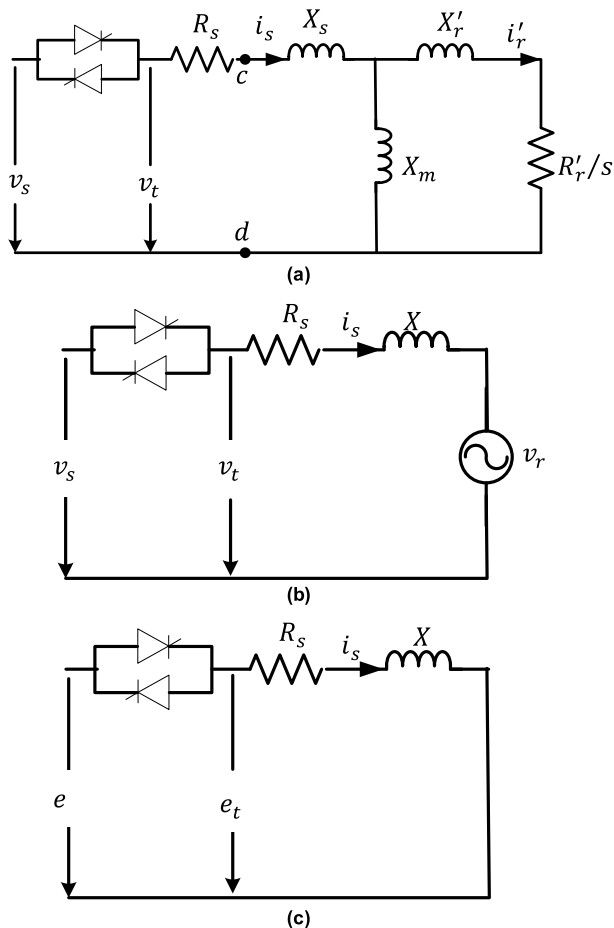
FIGURE 1. (a) Single-phase IM equivalent circuit. (b) Thevenin equivalent circuit. (c) RL equivalent circuit.

indicated in (3). The terminal voltage (V_t) depends on (α), while the voltage (V_r) depends mainly on the rotor back Electric Motive Force (E_r). Since the amplitude and phase of (E_r) vary with slip s (i.e. motor speed) and stator current (I_s) as given in (4)-(5), the stator current depends on the firing angle and motor speed. After defining the stator current, the rotor current and torque could be calculated as shown in (5)-(6).

$$V_r = E_r X_m / (X_m + X_r'), \tag{1}$$

$$X = X_s + X_m X_r' / (X_r' + X_m), \tag{2}$$

$$I_s = (V_t - V_r)/(R_s + X) \tag{3}$$

$$E_r = (R_r'/s) I_r', \tag{4}$$

$$I_r' = I_s X_m / (\sqrt{(R_r'/s)^2 + (X_m + X_r')^2}), \tag{5}$$

$$T_e = \frac{3 I_r'^2 R_r' (1\text{-}s)}{s \omega_r}, \tag{6}$$

where V_r and X are Thevenin equivalent voltage and reactance, respectively; I_r', R_r', and X_r' are rotor current, resistance, and leakage reactance referred to the stator circuit, respectively; X_m, T_e, s and ω_r are excitation reactance, electromagnetic torque, slip and rotor angular velocity, respectively.

In order to define the stator current, the Thevenin equivalent circuit is transformed to RL circuit because it is handy to handle with the RL circuit [27], [28]. The equivalent voltage (e) in the RL circuit is obtained by adding the supply and Thevenin equivalent voltages as follow: $e = v_s - v_r$. It is obviously clear that the Thevenin and RL circuits shown in Figs. 1-b & 1-c have the same stator current (i_s). However, the same current waveform has different firing angles (α_{th}) and (α_{RL}) because there is a phase difference (ξ) between the voltages (v_s) and (e) as shown in Fig. 2. Thus, the difference between the firing angles is equal to the phase shift between the two voltages as written in (7).
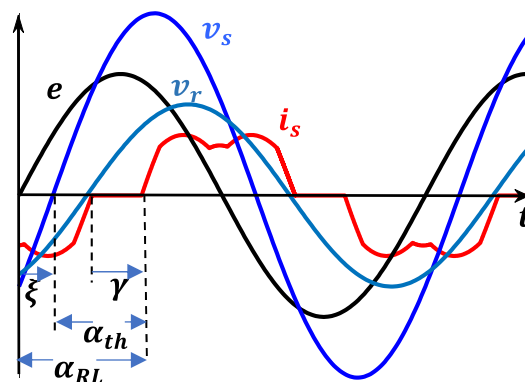
$$\alpha_{th} = \alpha_{RL} - \xi. \tag{7}$$

FIGURE 2. Voltages and current waveforms relationships.

For the RL circuit, the phase terminal voltage and stator current in both modes (2/3, 0/2) can be expressed in a Fourier series as follows:

$$e_t(t) = \sum_{h=1,2,...}^{\infty} \sqrt{a_h^2 + b_h^2} \sin(h\omega t + \varphi_h), \tag{8}$$

$$i_s(t) = \sum_{h=1,2,...}^{\infty} \frac{\sqrt{a_h^2 + b_h^2}}{z} \sin(h\omega t + \psi_h), \tag{9}$$

where a_h and b_h are the Fourier coefficients for each harmonic order h, $\varphi_h = \tan^{-1}\left(\frac{a_h}{b_h}\right)$, $z = \sqrt{R_s^2 + X^2}$, $\psi_h = \phi - \varphi_h$, and load angle $\phi = \tan^{-1}\left(\frac{X}{R_s}\right)$. For simplification, the fundamental components of the stator current and voltage are only considered since the other components are too small [27]. Therefore, the RMS stator current and its angle with the RMS voltage (E_1) can be written as follows:

$$I_s = \frac{\sqrt{a_1^2 + b_1^2}}{z\sqrt{2}}, \quad \psi_1 = \tan^{-1}\left(\frac{X}{R_s}\right) - \tan^{-1}\left(\frac{a_1}{b_1}\right). \tag{10}$$

The coefficients a_1 and b_1 are determined based on the voltage E_1, firing angle (α_{RL}) and hold off angle (γ). For example, for mode 2/3, the coefficients a_1 and b_1 can be

expressed in the following manner [28]:

$$a_1 = \frac{3E_1}{4\sqrt{2}\pi} \left(\cos\left(2\alpha_{RL}\right) - \cos\left(2(\alpha_{RL} - \gamma)\right) \right), \qquad (11)$$

$$b_1 = \frac{3E_1}{4\sqrt{2}\pi} \left(\sin\left(2\alpha_{RL}\right) - \sin\left(2(\alpha_{RL} - \gamma)\right) - 2\gamma + \frac{4\pi}{3} \right). \qquad (12)$$

From the phasor diagram shown in Fig. 3, the RMS voltage E_1 can be calculated as given in (13).

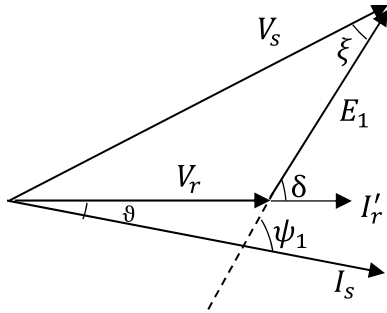$$E_1^2 = V_s^2 - V_r^2 - 2E_1 V_r \cos\delta. \qquad (13)$$

FIGURE 3. Phasor diagram of voltages and currents.

The phase shift (δ) between (E_1) and (V_r) as written in (14) is equal to the difference between the angles (ψ_1) and (ϑ). The angle (ψ_1) is the phase shift between (E_1) and (I_s) while the angle (ϑ) is the phase shift between (V_r) and (I_s).

$$\delta = \psi_1 - \vartheta, \qquad (14)$$

where $\vartheta = (\frac{\pi}{2} - \tan^{-1}((X_m + X_r')/(R_r'/s)))$. Applying the current boundary conditions in each mode, the angle (α_{RL}) can be obtained as a function of the hold off angle (γ) and load angle (ϕ). For example, α_{RL} can be determined for mode 0/2 by this formula [28]:

$$\alpha_{RL}$$
$$= \tan^{-1} \left(\frac{\sin\left(\phi + \gamma + \frac{\pi}{6}\right) + \sin\left(\phi - \frac{\pi}{6}\right)e^{R_s(\gamma - 2\frac{\pi}{3})/X}}{\cos\left(\phi + \gamma + \frac{\pi}{6}\right) + \cos\left(\phi - \frac{\pi}{6}\right)e^{R_s(\gamma - 2\frac{\pi}{3})/X}} \right). \qquad (15)$$

Using the motor parameters, the RMS of the supply voltage (V_s), and hold off angle (γ), equations (10) and (13) can be solved to get (E_1) and (I_s) at different motor speeds. After that, the angle (ξ) between the firing angles (α_{th}) and (α_{RL}) can be calculated as follows:

$$\xi = \cos^{-1}\left((E_1^2 + V_s^2 - V_r^2)/(2E_1 V_s)\right). \qquad (16)$$

The trial and error technique is used to solve the problem. At each pre-set motor speed (n), the angle (γ) is changed till obtaining a specified error between (α_{th}) and the pre-set value (α). At this error, n, α, and the corresponding torque (T_e) can be stored. The derived steps of getting the torque for different firing angles and motor speeds are illustrated in Algorithm. 1. As shown in Fig. 4, the torque-speed characteristic curves are deduced for different firing angles using the IM parameters given in Table. 1 (section V).
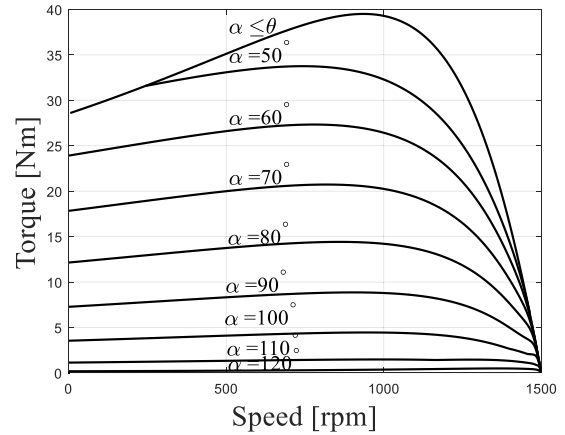
FIGURE 4. Torque variation with the motor speed and firing angle.

TABLE 1. IM parameters.

Parameter	Value	Parameter	Value
Rated Power	3 kW	Stator resistance	3 Ω
Rated voltage	380 V	Referred rotor resistance	3 Ω
Rated current	7.4 A	Stator leakage inductance	0.012 H
Rated frequency	50 Hz	Referred rotor leakage inductance	0.012 H
Rated load torque	20 Nm		
Rated speed	1400 rpm	Mutual inductance	0.30 H
Number of poles	4	Moment of inertia	0.034 kg.m^2

III. ANN-BASED SOFT STARTER CONTROLLER

To overcome the classic controller problems, the soft starting control scheme is developed using an ANN as a highly promising tool in the realm of intelligent control. ANN is inspired by the architecture and operation of biological nervous tissue. It could acquire knowledge and store information through learning processes [29], [30]. The feedforward and recurrent ANNs are the major structure classes. In the proposed acceleration control scheme, the ANN inputs are the motor speed and torque. The output firing angle depends mainly on the input present values i.e. the output is not function of the previous values. Therefore, the feedforward ANN is structurally convenient to be used. The feedforward ANN structure is organized into one input layer and one or more hidden layers, followed by an output layer. Each layer has a specific number of neurons. The number of hidden layers and neurons depends on the problem type and the required accuracy. Fig. 5 shows the necessary steps to train and develop a neural network with the help of MATLAB Neural Network Toolbox software. In the feedforward types, the back-propagation technique is normally used to adjust weights until the mean squared error (MSE) between the actual and ANN output patterns becomes small [30]. Once the desired error is obtained through the learning process, the numbers of ANN hidden layers and neurons are stored.

A MATLAB NN toolbox is used to develop the neural network model for the proposed control technique. The motor torque-speed characteristic curves for different firing angles shown in Fig. 4 are exploited in the training process.

Algorithm 1 Procedure of Obtained Motor Characteristics

1- **Input** motor parameters and RMS supply voltage V_s.
2- **Set** 1- the range of alpha $[\alpha_{min}, \alpha_{max}]$, speed $[n_{min}, n_{max}]$, and initial hold off angle $\gamma_{initial}$. 2- the increment $\Delta\alpha$, Δn and $\Delta\gamma$ and the required accuracy ϵ_{max}.
3- Initialize $\alpha = \alpha_{min}$.
4- Set $n = n_{min}$.
5- Set $\gamma = \gamma_{initial}$.
6- **If** $\gamma > \pi/3$, set mode 0/2
  Else set mode 2/3
  End
7- Define α_{RL} and voltage Fourier coefficients as a function of E_1 for the selected mode.
8- Solving equations (10) and (13) to get E_1 and I_s.
9- Calculate α_{th} and so, the error $\epsilon = \alpha_{th} - \alpha$
10- **If** $\epsilon > \epsilon_{max}$
    If $\epsilon < 0$
      $| \quad \gamma = \gamma + \Delta\gamma$
    Else
      $| \quad \gamma = \gamma - \Delta\gamma; \Delta\gamma = \Delta\gamma/2$
      $| \quad \gamma = \gamma + \Delta\gamma$
    END
    Go to step 6
  Else
    Calculate I'_r and T_e as shown in (5) and (6).
    Store α, n, T_e.
    Set $n = n + \Delta n$
    If $n < n_{max}$
      $| \quad$ Go to step 5
    Else
      $| \quad \alpha = \alpha + \Delta\alpha$
      If $\alpha < \alpha_{max}$
        $| \quad$ Go to step 4
      Else
        $| \quad$ Stop
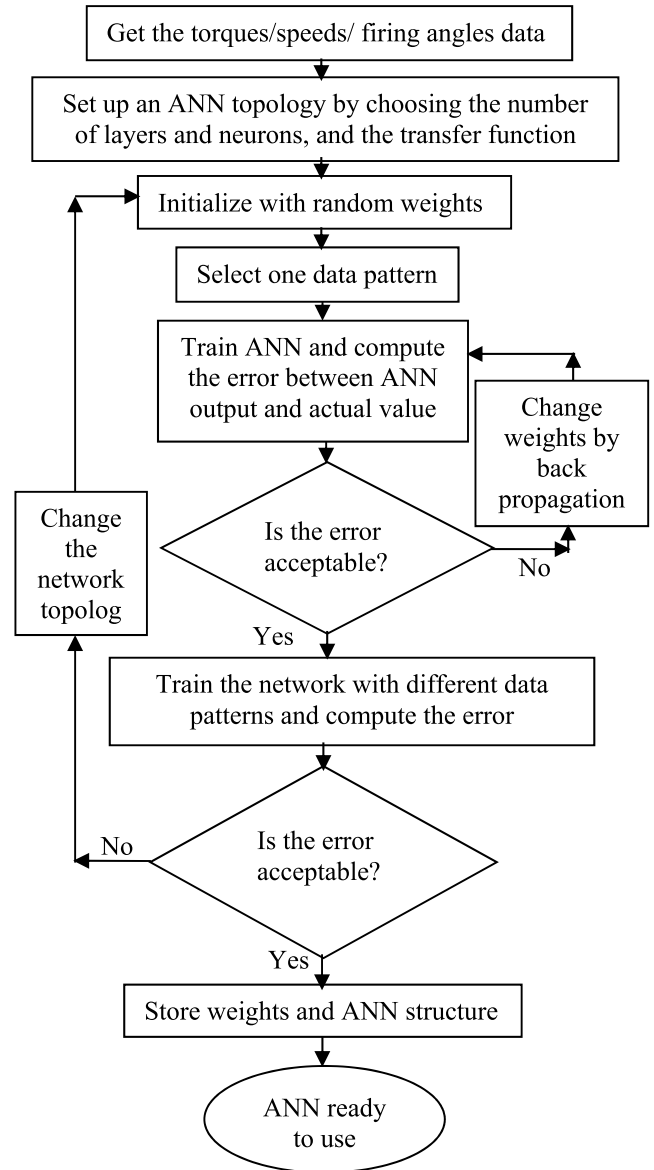   **END**
    END
  END
END

FIGURE 5. Neural network design flow chart.

70% of the data is used for the training process, 15% is used for validation and 15% is used for testing. To represent the nonlinear relationship among variables, Tan sigmoidal function is used to characterize the transfer function of the hidden layers as given in (17). While Pureline function signifies the output layer transfer function. The structure of ten neurons in one hidden layer achieves the required accuracy (MSE = 0.0001) on training time (9 mins).

$$\varphi(s) = \frac{2}{1 + e^{-2s}} - 1. \tag{17}$$

IV. SYSTEM DESCRIPTION

The schematic diagram of the IM- soft starter model is shown in Fig. 6. The model consists of a three-phase IM, three pairs

back-to-back thyristors, firing control system and data measurement system. The IM voltage is controlled by adjusting the thyristors firing angle (α) with respect to the zero crossing of the supply voltage. The thyristors are selectively fired to conduct an adopted phase current, and naturally commutated off when the current reaches to zero. RC snubber circuit is incorporated to reduce the switching transients of the commutation process. The firing control system contains three voltage transducers, shifting circuit, DSP board, and gate drive circuit. The LEM Module LV 25-P voltage transducer is used to step down the supply voltage to ±1.5V. It can also provide an electrical isolation between the power circuit and DSP controller. Since the analog inputs of the DSP board accept only signals ranged from 0V to 3V, a shifting circuit is designed to shift the AC outputs of the voltage transducers to a unidirectional voltage. A 1.5V DC offset circuit
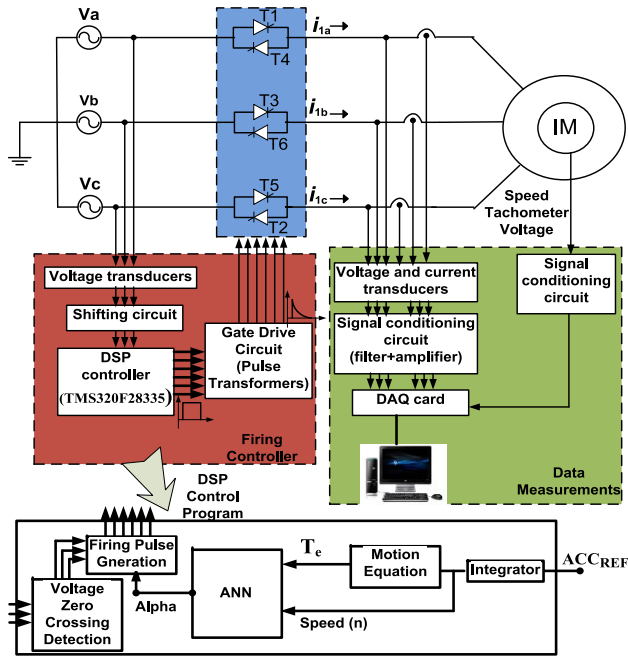
FIGURE 6. Soft starter fed IM Schematic diagram.

is used to provide the essential DC offset to the measured AC signals (±1.5V).

As a main processing unit of the firing control circuit, a Texas Instrument (Model: TMS320F28335) DSP controller board is utilized to control the switching sequences of the thyristor switches. Using a MATLAB code, the zero-crossing detection (ZCD) algorithmis programmed to detect the zero crossing of the supply voltages feeding into the analog inputs of the DSP board. Then, the code composer studio software is employed to download the ZCD and ANN control algorithms into the DSP board. The ANN controller adjusts the output of firing angle depending on the inputs of IM torque and speed. The motor speed is determined from the integration of the reference acceleration (ACC$_{REF}$), while the torque is estimated from the motion equation given in (18) based on the defined load torque and required accelerating torque. After defining the firing angle, the DSP board generates the digital firing pulses with respect to the voltage zero crossing and sends to the gate drive circuit. Pulse transformers are involved in the gate drive circuit to provide sufficient currents for turning-on the thyristors. They are also used to isolate electrically between the high and low power stages of the thyristors.

$$T_e = T_L + T_{acc},$$
$$T_{acc} = J\,(d\omega_r/dt) + f\,\omega_r, \qquad (18)$$

where T_{acc} is the accelerating torque, $(d\omega_r/dt)$ is the motor acceleration, T_L is the load torque, J is the moment of inertia of the rotor and load, and f is the viscous friction and windage coefficient.

The data measurement system consists of voltage and current transducers, signal conditioning circuits, and DAQ board

from USB-6229 National Instrument. Sixteen analog inputs can be acquired by this board at a sampling rate of 250 k samples/sec and 16-bit resolution. The high sampling rate and high resolution of the DAQ board allow the user to obtain a very precise and accurate data structures. The signals from the motor terminal voltages transducers, line currents transducers, and speed tachometer must be conditioned using the signal conditioning circuit to shield the signals from the noise and distortion. To be monitored on LabVIEW software, the real-time data are fed into the analog inputs of the DAQ board plugged in the computer board. The software consists of a front panel and block diagram. As a graphical user interface, the front panel is used to display the data. While the block diagram is used to show the process of the displayed mechanics in the front panel.

V. SIMULATION RESULTS

The model of IM- soft starter system has been designed and implemented in MATLAB/SIMULINK to investigate the proposed soft starting control scheme. The case study motor used in simulation is a laboratory 3 kW, Y-connected three-phase wound rotor IM. The equivalent circuit parameters for the IM are given in Table 1. First, the actual firing angles have been compared with the obtained ANN firing angles as shown in Fig. 7 to investigate the accuracy of the designed ANN model. A good fitting between the ANN and actual results has been clearly observed. The comparison data differ from the training data. Then, the effectiveness of the proposed control technique has been verified. To steadily increase the IM speed, the IM acceleration (speed rate) has kept constant during the starting period. As a result, the reference motor speed (n) calculated from the integration of the reference acceleration is a ramp function. The firing angle has been determined from the ramp reference speed and estimated motor torque T_e given in (18). The proposed ANN-based acceleration control scheme has been compared with the direct online starting (DOL) scheme to demonstrate the advantages of the proposed acceleration control.
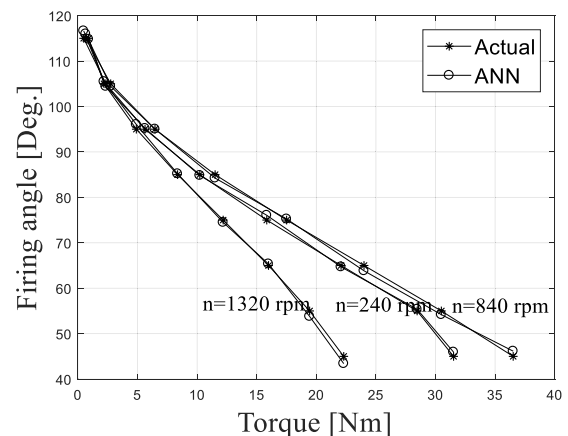

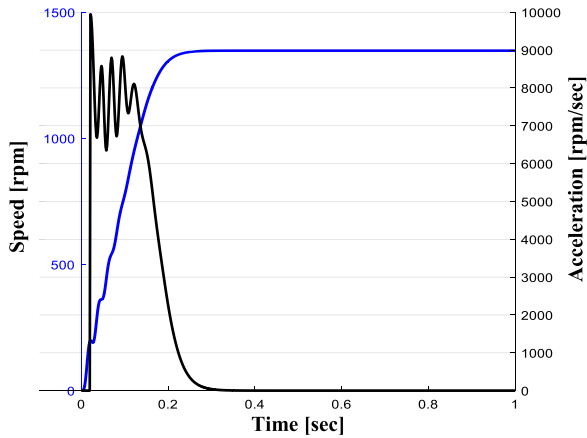**FIGURE 7.** Comparison between actual and ANN output firing angles.

FIGURE 8. Motor speed and acceleration time responses for DOL technique under the rated pump load condition.
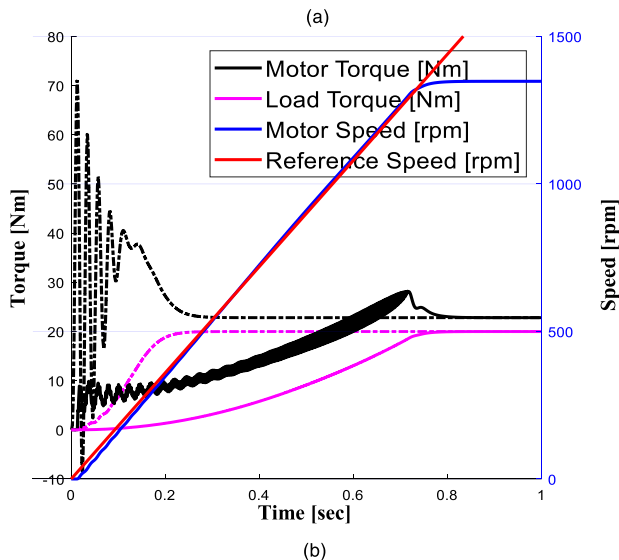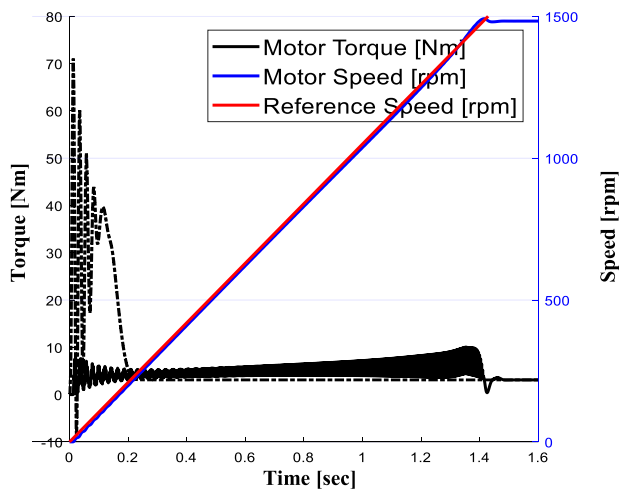

(a)

(b)

FIGURE 9. Motor speed and electromagnetic torque time responses for DOL (dash line) and acceleration control techniques (solid line) (a) under no-load and (b) the rated pump load conditions.

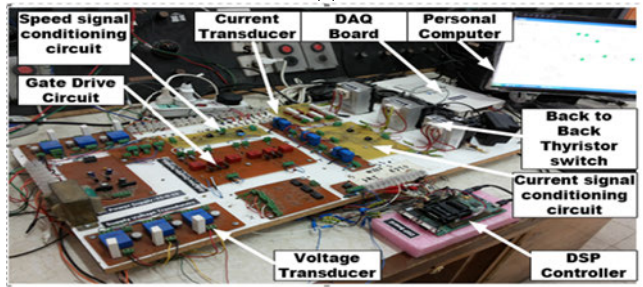In the DOL, the high variation of motor acceleration is clearly shown in the acceleration time response in Fig. 8.

(a)

(b)

FIGURE 10. Experiment setup configurations (a) setup machines; (b) soft starter and its control circuit.

It soars to about 10^4 rpm/sec, which causes mechanical stress on the drive components like gears, belts and chains. Fig. 9 depicts the starting performance of the motor with the proposed acceleration controller under no-load condition at 1000 rpm/sec reference acceleration and rated pump load condition at 1800 rpm/sec reference acceleration. A pumped load function $0.001\omega_r^2$ [Nm] is used. The results show a good tracking between the actual motor speed and reference speed profile. With the proposed controller, the IM torque has been controlled to follow the load torque variation preserving the motor acceleration constant at the reference value.

VI. EXPERIMENTAL RESULTS

A laboratory prototype of the IM- soft starter system is shown in Fig. 10. The prototype includes a motor-generator rig and soft starter circuit. Due to the laboratory facilities, a 1.5 kW DC generator is used as a mechanical load to provide an approximately half-rated load torque at steady state speed. Therefore, the experimental works have been accomplished at this half load $4.5 + 0.038\omega_r$ [Nm]. To experimentally validate the motor characteristics obtained in section II, the theoretical and experimental results have been compared for different firing angles and loading conditions. Fig. 11 shows the steady state voltage and current waveforms of the IM for both theoretical and experimental works. It can be clearly noticed from the comparison that the theoretical and experimental results are in good agreement. Their magnitudes and waveforms profiles are quite close. The slight difference between the results is due to the digital measurement system. In addition, the voltage and current transducers and/or the data acquisition board cause small DC offsets.

To investigate the effectiveness of the proposed acceleration control scheme, a series of experimental tests with various reference accelerations has been conducted under
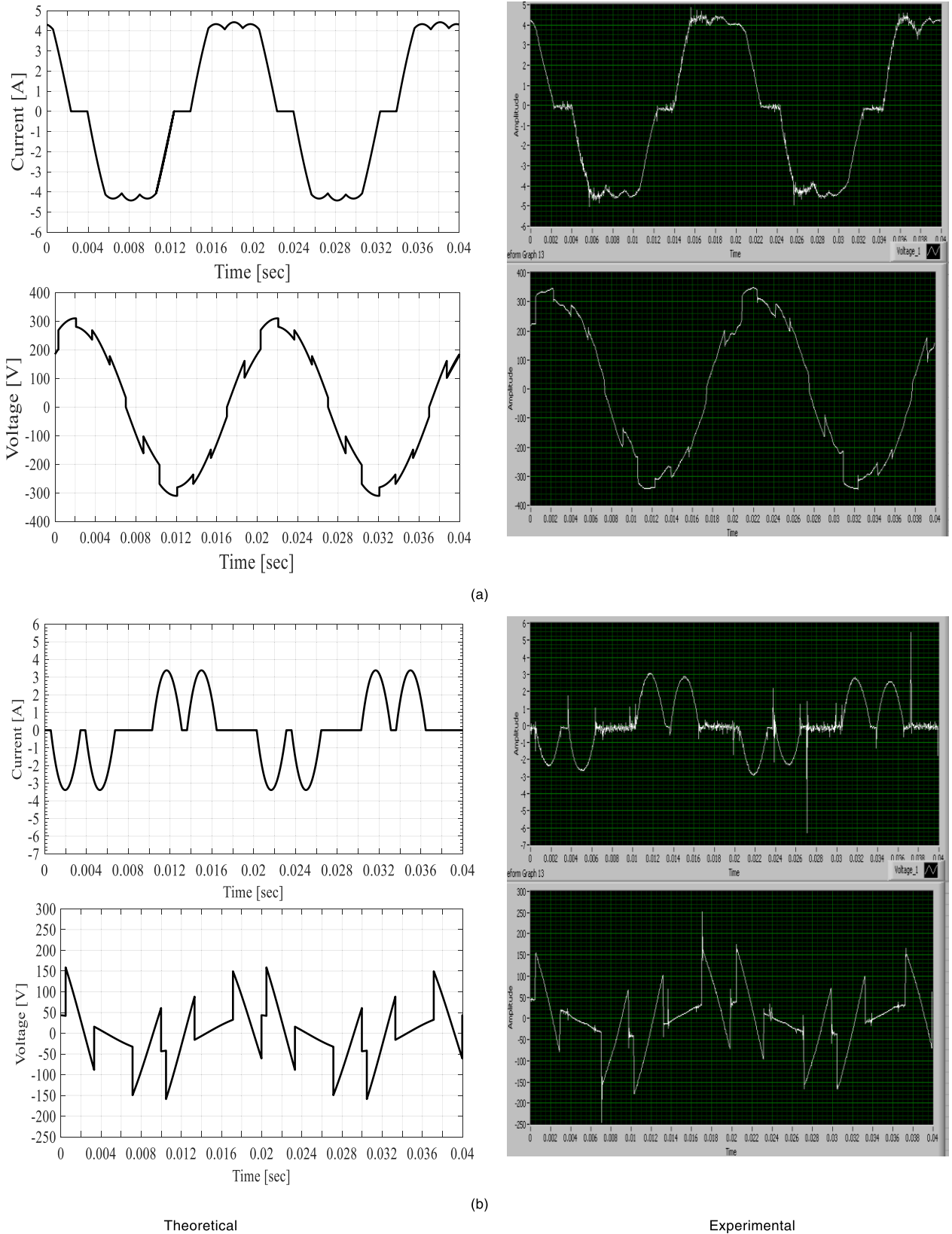
FIGURE 11. The IM theoretical and experimental waveforms of stator current and terminal phase voltage at: (a) motor speed of 1440 rpm and $\alpha = 60°$; (b) motor speed of 1300 rpm and $\alpha = 115°$.
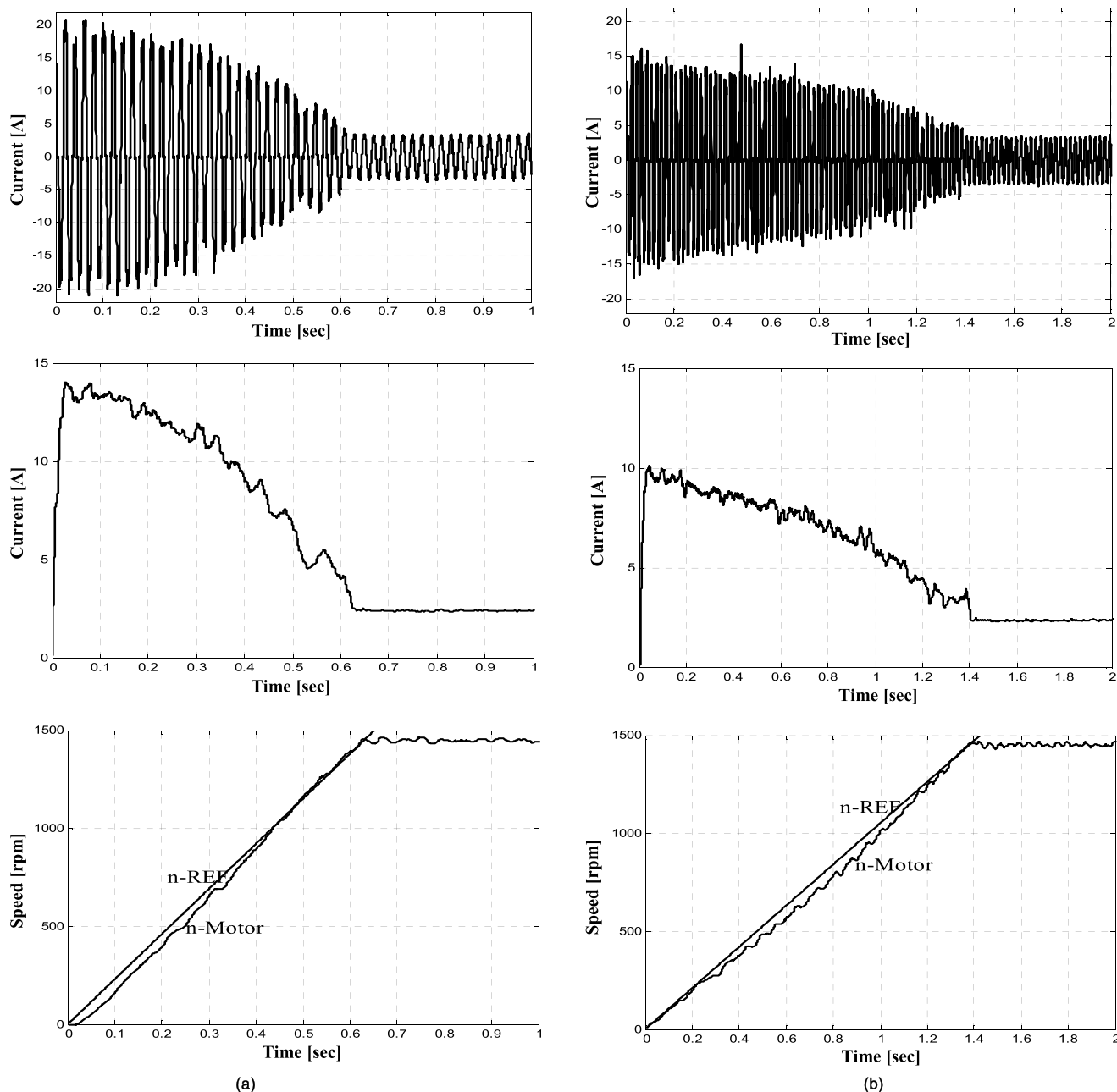
FIGURE 12. Instantaneous and its RMS starting current, and speed of the IM vs. time under no-load condition at: (a) 2300 rpm/sec reference acceleration; (b) 1050 rpm/sec reference acceleration.

two different loading conditions. Firstly, Fig. 12 illustrates the IM instantaneous stator current, its computed RMS current, and motor speed under no-load condition and reference accelerations of 1050 and 2300 rpm/sec. Secondly, the system performance has been checked under half-load condition and reference accelerations of 900 and 1600 rpm/sec as shown in Fig. 13. The results indicate that the actual motor speed is experimentally quite closed to the reference speed profile calculated from the integration of the reference acceleration. In terms of the low starting current and the low rate of speed during the starting period, the proposed control scheme is showing an excellent starting performance for the

three-phase IM under different reference accelerations and loading conditions. It is worth mentioning that increasing the reference acceleration decreases the acceleration time. Therefore, a good compromise between the detected reference acceleration and acceleration time should be considered.

VII. RESULTS DISCCUSION AND COMPARISON WITH PREVIOUS WORKS

As shown in simulation and real-time results, the proposed control scheme has been compared with the DOL scheme under no-load, pump load and half-load conditions. DOL has been selected for comparison because it produces the highest
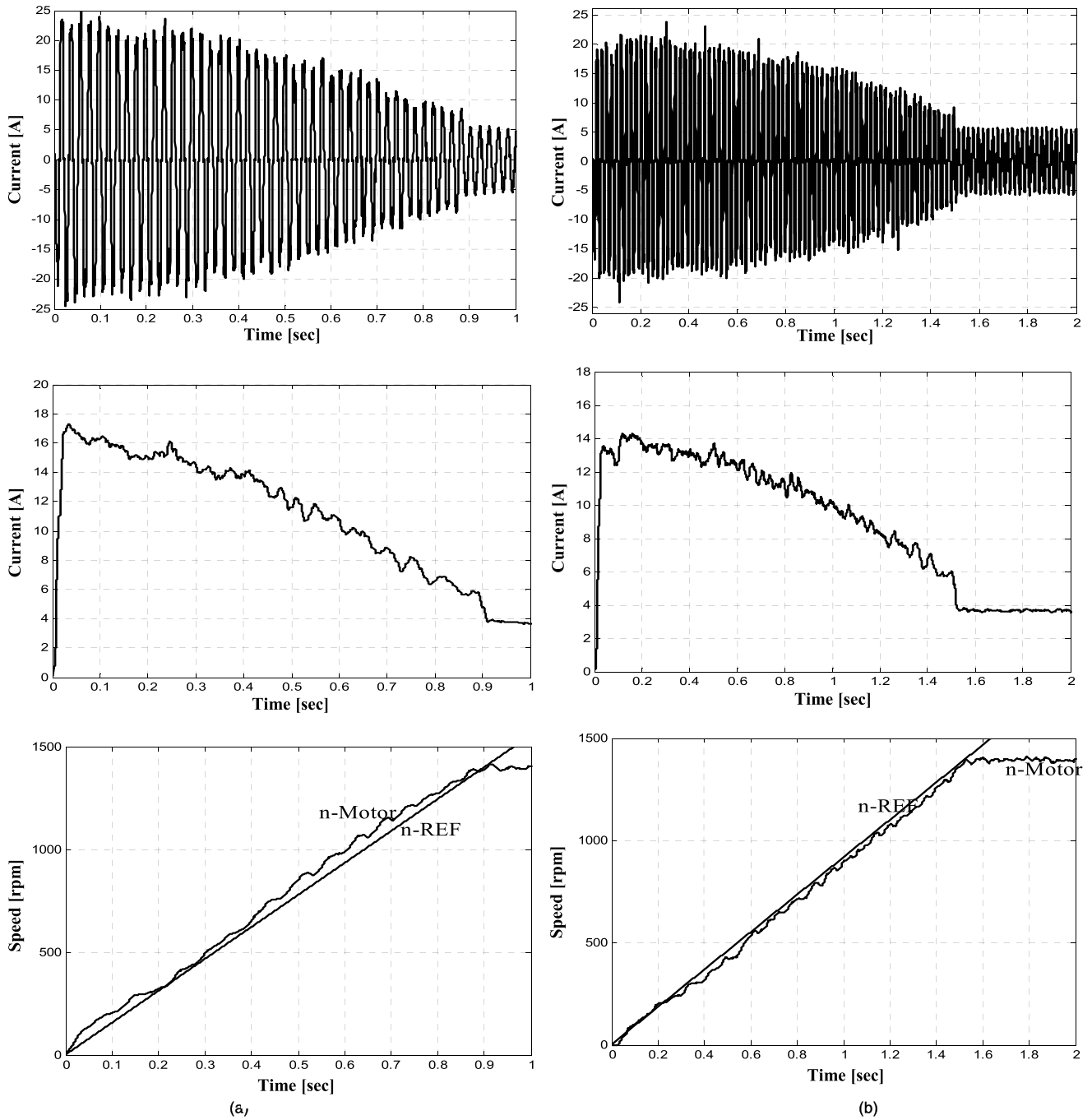
FIGURE 13. Instantaneous and its RMS starting current, and speed of the IM vs. time under half-load condition at: (a) 1600 rpm/sec reference acceleration; (b) 900 rpm/sec reference acceleration.

inrush current (four to eight times the rated current) and largest accelerating torque [2]. Moreover, other starting techniques are mostly baselined against it. In the DOL, the maximum RMS starting current and acceleration time under no-load condition are about 28A and 0.21 sec, respectively as shown in Fig. 14. For half-load condition, the maximum RMS starting current and acceleration time are 29A and 0.25 sec. Using the proposed acceleration control scheme, the maximum RMS starting current is decreased nearly to 14A and 17A at reference accelerations of 2300 rpm/sec

and 1600 rpm/sec under no-load and half-load conditions, respectively as depicted in Figs. 12 & 13. This means that the controller can lower the maximum RMS starting current of the DOL by 50% and 41% at the no-load and half-load conditions, respectively, with a reasonable increase in the acceleration time (i.e. 0.42 sec and 0.67 sec, respectively). In addition, from the simulation results shown in Figs. 8 & 9, the acceleration control scheme can control the motor torque to follow the load torque variation keeping the accelerating torque constant at level based on the reference acceleration
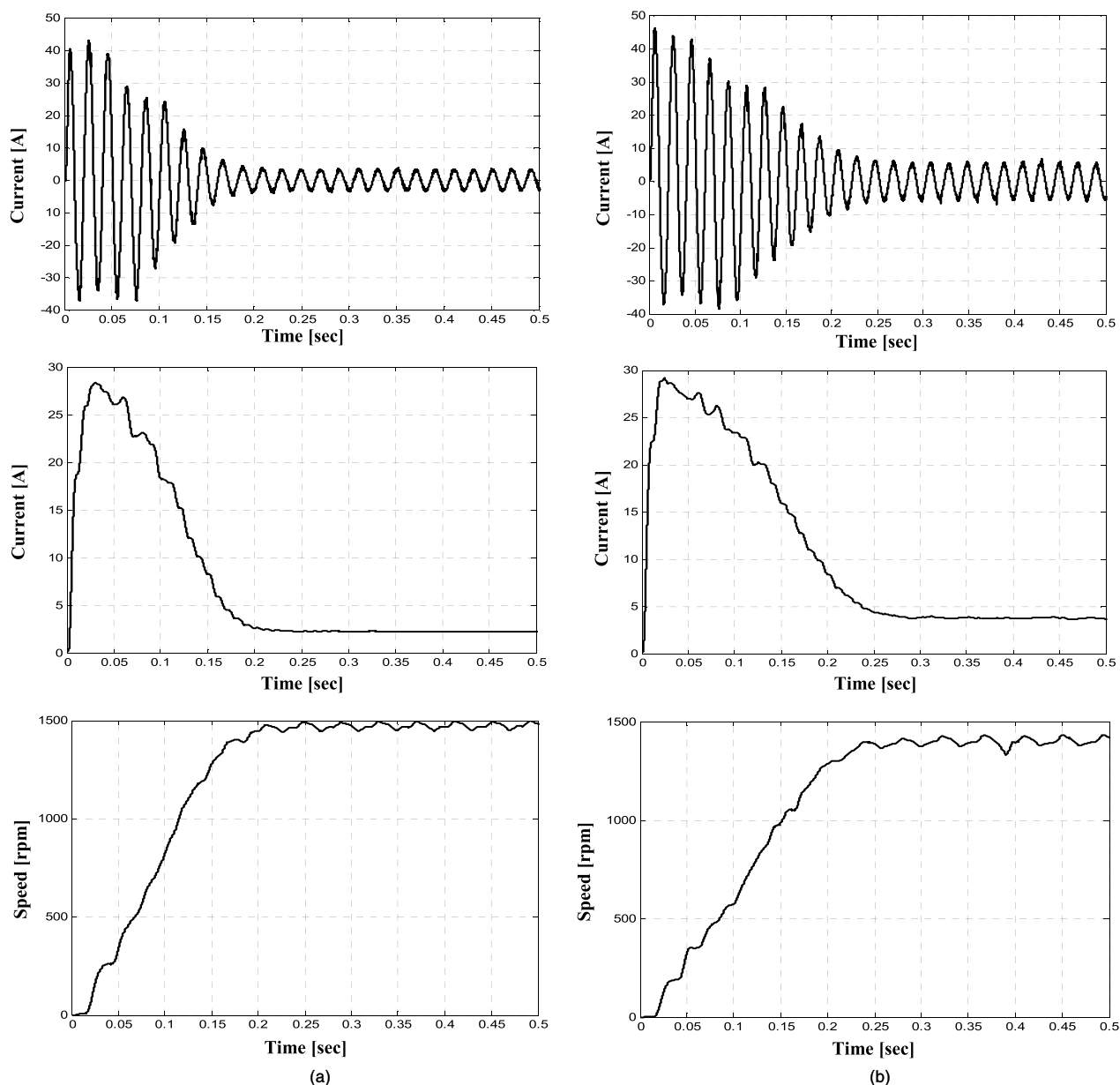
FIGURE 14. Instantaneous and its RMS starting current, and speed of the IM vs. time for DOL at: (a) no-load condition; (b) half-load condition.

value. The high variation of the motor acceleration at the DOL technique is prevented. The DOL maximum acceleration and acceleration time are 10^4 rpm/sec and 0.28, respectively at the pump load condition. While their counterparts are 1800 rpm/sec and 0.8 sec for the acceleration controller. Consequently, the maximum acceleration of the DOL is remarkable decreased by 82% with an increased acceleration time of 0.52 sec. Furthermore, the high pulsations clearly shown in the time response of DOL electromagnetic torque are minimized using the acceleration control technique.

Table 2. illustrates a detailed comparison between the proposed control scheme and previous soft starting control schemes of the three phase IM. This comparison is based on the art of control, sensor requirements, control algorithm complexity, and the processor cost. It is concluded that the soft starting methods presented in literature [11]–[13], [24] need a high number of voltage and current sensors. Moreover, their control circuits are complicated. In the proposed soft starting method, the acceleration is used as the control parameter. Therefore, the control circuit configuration becomes an open loop. There is no need for the motor current feedback as proposed in [12], [13] or estimated torque feedback as [24]. It requires only three voltage sensors for detecting the zero crossing of the supply voltages. Moreover, the challenges of tuning the PI controller parameters [24] and testing different time functions of firing angle variation [11]–[13] are settled. Using ANN approach, the control algorithm has become simple. Therefore, a low-cost processor can be utilized for

TABLE 2. Comparison between the proposed control scheme and previous works.

Control schemes of soft starter	Control parameter	Control type	Sensors count (V: voltage and I: current)	Firing angle variation	Algorithm complexity	Cost of the used processor
[11]	voltage	open loop	3-V& 3-I	Time function	moderate	moderate
[12-13]	current	closed loop	3-V& 1-I	Time function	moderate	moderate
[24]	torque	closed loop	6-V& 3-I	PI controller	high	high
The proposed control scheme	acceleration	open loop	3-V	ANN controller	low	low

executing the control algorithm due to its low computational burden.

VIII. CONCLUSION

A novel acceleration control scheme based on ANN has been investigated for soft-starter fed three-phase IM. The proposed acceleration controller was simulated and experimentally validated on a laboratory 3-kW IM soft-starter system. A series of simulation and real-time tests were carried out to validate the effectiveness of the controller under different loading conditions. The results prove the reliability of the acceleration control scheme under different reference accelerations and loading conditions. Compared with the DOL starting scheme, the acceleration controller can lower the maximum RMS starting current by 50% and 41% at the no-load and half-load conditions, respectively, with a reasonable increased acceleration time (i.e. 0.42 sec and 0.67 sec, respectively). In addition, the controller can decrease the DOL maximum acceleration by nearly 77% and 84% at the no-load and half-load conditions, respectively. Therefore, the IM can be started smoothly with neither electrical stress on the supply utility nor mechanical stress on the drive components like gears, belts, and chains. Moreover, employing the ANN approach makes the acceleration controller preferred compared with several soft starting control schemes. It has a simple control algorithm, less required sensors, and uncomplicated control circuit configuration. Hence, a low-cost processor can be used in the industrial implementation of the proposed control system.

REFERENCES

[1] R. F. McElveen and M. K. Toney, "Starting high-inertia loads," *IEEE Trans. Ind. Appl.*, vol. 37, no. 1, pp. 137–144, Jan./Feb. 2001.

[2] J. Larabee, B. Pellegrino, and B. Flick, "Induction motor starting methods and issues," in *Proc. Rec. Conf. Papers Ind. Appl. Soc., 52nd Annu. Petroleum Chem. Ind. Conf.*, 2005, pp. 217–222.

[3] C. Yang, S. Park, S. B. Lee, G. Jang, S. Kim, G. Jung, J. Lee, S. Shim, Y. K. Lim, and J. Kim, "Starting current analysis in medium voltage induction motors: Detecting rotor faults and reactor starting defects," *IEEE Ind. Appl. Mag.*, vol. 25, no. 6, pp. 69–79, Nov. 2019, doi: 10.1109/MIAS.2019.2923105.

[4] M. Akbaba, "A novel simple method for elimination of DOL starting transient torque pulsations of three-phase induction motors," *Eng. Sci. Technol., Int. J.*, to be published, doi: 10.1016/j.jestch.2020.06.007.

[5] C.-C. Yeh and N. A. O. Demerdash, "Fault-tolerant soft starter control of induction motors with reduced transient torque pulsations," *IEEE Trans. Energy Convers.*, vol. 24, no. 4, pp. 848–859, Dec. 2009.

[6] S. A. Deraz and H. Z. Azazi, "Current limiting soft starter for three phase induction motor drive system using PWM AC chopper," *IET Power Electron.*, vol. 10, no. 11, pp. 1298–1306, Sep. 2017.

[7] F. Jiang, C. Tu, Q. Guo, Z. Wu, and Y. Li, "Adaptive soft starter for a three-phase induction-motor driving device using a multifunctional series compensator," *IET Electr. Power Appl.*, vol. 13, no. 7, pp. 973–983, Jul. 2019.

[8] Y. Wang, K. Yin, Y. Yuan, and J. Chen, "Current-limiting soft starting method for a high-voltage and high-power motor," *Energies*, vol. 12, no. 16, pp. 3068–3079, 2019.

[9] N. G. Furtsev, A. S. Petrikov, and A. N. Belyaev, "Optimizing soft starter algorithms for heavy induction motors to ensure stable operation of autonomous power systems," in *Proc. IEEE Conf. Russian Young Researchers Electr. Electron. Eng. (EIConRus)*, St. Petersburg Moscow, Russia, Jan. 2020, pp. 1222–1226, doi: 10.1109/EIConRus49466.2020.9039488.

[10] V. Thanyaphirak, V. Kinnares, and A. Kunakorn, "Comparison of starting current characteristics for three-phase induction motor due to phase-control soft starter and asynchronous PWM AC chopper," *J. Electr. Eng. Technol.*, vol. 12, no. 3, pp. 1090–1100, May 2017.

[11] M. G. Solveson, B. Mirafzal, and N. A. O. Demerdash, "Soft-started induction motor modeling and heating issues for different starting profiles using a flux linkage ABC frame of reference," *IEEE Trans. Ind. Appl.*, vol. 42, no. 4, pp. 973–982, Jul. 2006.

[12] G. Zenginobuz, I. Cadirci, M. Ermis, and C. Barlak, "Performance optimization of induction motors during voltage-controlled soft starting," *IEEE Trans. Energy Convers.*, vol. 19, no. 2, pp. 278–288, Jun. 2004. 10.1109/TEC.2003.822292

[13] P. M. Shabestari and A. Mehrizi-Sani, "Current limiting and torque pulsation reduction of the induction motors," in *Proc. IEEE Power Energy Soc. Gen. Meeting (PESGM)*, Aug. 2019, pp. 1–5.

[14] M. Ghadimi, A. Ramezani, and M. Mohammadimehro, "Soft starter modeling for an induction drive starting study in an industrial plant," in *Proc. 5th Eur. Symp. Comput. Modeling Simulation (UKSim)*, Nov. 2011, pp. 245–250.

[15] S. Pandey, S. Bahadure, K. Kanakgiri, and N. M. Singh, "Two-phase soft start control of three-phase induction motor," in *Proc. IEEE 6th Int. Conf. Power Syst. (ICPS)*, Mar. 2016, pp. 1–6.

[16] K. Sundareswaran and P. S. Nayak, "Ant colony based feedback controller design for soft-starter fed induction motor drive," *Appl. Soft Comput.*, vol. 12, no. 5, pp. 1566–1573, May 2012.

[17] K. Sundareswaran and P. Srinivasarao, "Design of feedback controller for soft-starting induction motor drive system using genetic algorithm," *J. Ind. Electron. Drives*, vol. 1, no. 2, pp. 111–120, 2014.

[18] K. Sundareswaran and P. Nayak, "Particle swarm optimisation based feedback controller design for induction motor soft-starting," *Austral. J. Electr. Electron. Eng.*, vol. 11, no. 1, pp. 55–63, 2014.

[19] M. Mohanty, S. K. Sahu, M. R. Nayak, A. Satpathy, and S. Choudhury, "Application of salp swarm optimization to pi controller to mitigate transients in a three-phase soft starter-based induction motor," in *Advances in Electrical Control and Signal Systems*, vol. 665. Singapore: Springer, 2020.

[20] P. S. R. Nayak and T. A. Rufzal, "Performance analysis of feedback controller design for induction motor soft-starting using bio-inspired algorithms," in *Proc. Int. Conf. Power, Instrum., Control Comput. (PICC)*, Jan. 2018, pp. 1–6.

[21] P. S. R. Nayak and T. A. Rufzal, "Flower pollination algorithm based PI controller design for induction motor scheme of soft-starting," in *Proc. 20th Nat. Power Syst. Conf. (NPSC)*, Dec. 2018, pp. 1–6.

[22] Z. Ze and H. H. Ming, "Soft starter study of induction motors using fuzzy PID control," in *Proc. IOP Conf., Mater. Sci. Eng.*, vol. 439, 2018, Art. no. 032115.

[23] T. C. Mallick, S. Dhar, and J. Khan, "Artificial neural network based soft-starter for induction motor," in *Proc. 2nd Int. Conf. Electr. Inf. Commun. Technol. (EICT)*, Dec. 2015, pp. 228–233.

[24] A. Nied, J. de Oliveira, R. de Farias Campos, R. P. Dias, and L. C. de Souza Marques, "Soft starting of induction motor with torque control," *IEEE Trans. Ind. Appl.*, vol. 46, no. 3, pp. 1002–1010, Jun. 2010.

[25] M. A. Saqib and A. R. Kashif, "Soft starter of an induction motor using neural network based feedback estimator," in *Proc. Austr. Univ. Power Eng.*, 2007, pp. 1–5.

[26] S. A. R. Kashif and M. A. Saqib, "A neuro fuzzy application: Soft starting of induction motors with reduced energy losses," *Electr. Power Compon. Syst.*, vol. 40, no. 12, pp. 1339–1350, Aug. 2012.

[27] C.-C. Yeh, "Fault tolerant operations of induction motor-drive systems," Ph.D. dissertation, Dept. Elect. Comput. Eng., Marquette Univ., Milwaukee, WI, USA, May 2008.

[28] S. A. Hamed and B. J. Chalmers, "Analysis and performance of a three-phase thyrode voltage regulator supplying R-L loads," *Electr. Mach. Power Syst.*, vol. 15, nos. 4–5, pp. 209–230, Dec. 1988.

[29] M.-H. Kim, M. G. Simoes, and B. K. Bose, "Neural network-based estimation of power electronic waveforms," *IEEE Trans. Power Electron.*, vol. 11, no. 2, pp. 383–389, Mar. 1996.

[30] B. Karanayil and M. F. Rahman, "Artificial neural network applications in power electronics and electric drives," in *Power Electronics Handbook*. Amsterdam, The Netherlands: Elsevier, 2018, pp. 1245–1260.

AMIR ABDEL MENAEM received the B.S. and M.S. degrees in electrical engineering from Mansoura University, Egypt, in 2008 and 2014, respectively. He is currently pursuing the Ph.D. degree in electrical engineering with the Ural Energy Institute, Ural Federal University, Yekaterinburg, Russia. His field of interests include power electronics, artificial intelligence techniques, power system operation, planning of hybrid renewable energy systems, and uncertainty analysis, renewable distributed generations, and optimization techniques.

MOHAMED ELGAMAL (Graduate Student Member, IEEE) received the B.S. and M.S. degrees in electrical engineering from Mansoura University, Egypt, in 2009 and 2014, respectively, where he is currently pursuing the Ph.D. degree in electrical engineering. His field of interests include smart grids, microgrids, and artificial intelligence techniques, multiagent control systems, power system operation, and control of renewable energy systems.

ABDEL-HALEEM ABDEL-ATY received the B.Sc. and M.Sc. degrees in physics from the Department of Physics, Al-Azhar University, Egypt, in 2004 and 2009, respectively, the master's degree and the Ph.D. degree in theoretical physics (quantum information) from Universiti Teknologi Petronas, Malaysia, in 2011 and 2015, respectively. His Ph.D. study was supported by a Scholarship from Universiti Teknologi Petronas. In 2015, he received the Sultana Nahar's Prize for the best Ph.D. thesis in Egypt. In 2017, he received a scholarship as a Visiting Researcher with the University of Oxford, U.K. In 2017, has been elected as a Junior Associate Member at the African Academy of Science, Kenya. He is especially working in theories of quantum measurement, nanomechanical modeling, highly non-classical light, practical information security, and optical implementations of quantum information tasks. His current research interests include quantum resources, optical and atomic implementations of quantum information tasks and protocols, quantum computing, mathematical modeling, computational intelligence, and machine learning. He has authored or coauthored more than 60 articles in ISI journals, four book chapters and ten papers in conference proceedings and indexed by Scopus and ISI. He is acting as a Managing Editor of some journals, such as *Information Sciences Letters* (Scopus), *Quantum Physics Letters*, and the *International Journal of New Horizons in Physics*, and a Vice President of Natural Sciences Publishing, USA.
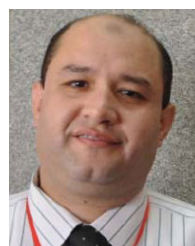
EMAD E. MAHMOUD was born in Sohag, Egypt, in 1975. He received the B.Sc. degree (Hons.) in mathematics from South Valley University in 2004 and the M.Sc. degree and the Ph.D. degree in dynamical systems from Sohag University, Sohag, Egypt, in 2007 and 2010, respectively. He has authored or coauthored over 70 articles in international refereed journals and two books in Lambert Academic Publishing. The areas of interest are synchronization and control of nonlinear dynamical systems (complex systems) and nonlinear differential equations.

ZHE CHEN (Fellow, IEEE) received the B.Eng. and M.Sc. degrees in electrical engineering from the Northeast China Institute of Electric Power Engineering, Jilin, China, the M.Phil. degree in power electronic from Staffordshire University, U.K., and the Ph.D. degree in power and control from the University of Durham, U.K. He has been a Full Professor with the Department of Energy Technology, Aalborg University, Denmark, since 2002. He is the Leader of Wind Power System Research Program with the Department of Energy Technology, Aalborg University, and the Danish Principle Investigator for Wind Energy of Sino-Danish Centre for Education and Research. He has led and participated in many research and industrial projects and has been a panel member of research funding evaluation committees in many EU countries. His research areas are power systems, power electronics, electric machines, wind energy, and modern power systems. He is a member of editorial boards for many international journals, a Fellow of the Institution of Engineering and Technology, London, U.K., and a Chartered Engineer in the U.K. He is an Associate Editor of the IEEE TRANSACTIONS ON POWER ELECTRONICS.

MOHAMED A. HASSAN (Member, IEEE) was born in Mansoura, Egypt. He received the B.Sc. degree (Hons.) and the M.Sc. degree in electrical engineering from Mansoura University, Mansoura, Egypt, in 1995 and 2000, respectively, and the Ph.D. degree from the King Fahd University of Petroleum and Minerals (KFUPM), Dhahran, Saudi Arabia, in 2011. He was with the Department of Electrical Engineering, Mansoura University, Mansoura, Egypt, as an Assistant Professor, from 2012 to 2018, where he has been an Associate Professor since 2018. He is currently on leave from Mansoura University. He is currently a Research Engineer III with the Center of Engineering, Research Institute, KFUPM. His current research interests include power electronics, microgrids, power system control, and operation and optimization techniques applied to power systems.

• • •